"RADIATION-INDUCED SEGRETATION AND THE RELATIONSHIP TO PHYSICAL PROPERTIES IN IRRADIATED AUSTENTIC ALLOYS"

By

T.R. Allen, J.I. Cole, G.S. Was*, and E.A. Kenik**

Nuclear Technology Division
Argonne National Laboratory-West
P. O. Box 2528
Idaho Falls, ID 83403-2528

*University of Michigan
Ann Arbor, MI 48109

**Oakridge National Laboratory
P. O. Box 2008
Oak Ridge TN 37831

To be Presented
at
National Society of Black Physicists Conference Procedings

Huntsville Alabama
March 13 – 16, 2002

*Work supported by the U.S. Department of Energy, Office of Nuclear Energy, Science and Technology, under Contract W-31-109-ENG-38.

Radiation-induced Segregation and the Relationship to Physical Properties in Irradiated Austenitic Alloys

T. R. Allen*, J. I. Cole, G. S. Was, and E. A. Kenik

Radiation-induced changes in composition are studied because these changes can degrade failure of materials irradiated in nuclear reactors. In this work, the effect of alloy composition on radiation-induced segregation, hardening, and void swelling is presented. Five alloys, Fe-18Cr-8Ni, Fe-16Cr-13Ni, Fe-18Cr-40Ni, Fe-16Cr-13Ni+Mo, and Fe-16Cr-13Ni+Mo+P (all compositions in wt. %), were irradiated with 3.2 MeV protons at 400°C to a dose of 0.5 displacements per atom. The change in grain boundary composition was measured using field emission gun scanning transmission electron microscopy and the hardening was measured using Vickers indentation. Void swelling is calculated from the void size distribution measured using transmission electron microscopy. After irradiation, Cr depletes and Ni enriches at grain boundaries. Increasing bulk Ni concentration causes greater Cr depletion and Ni enrichment at grain boundaries. For alloys with 16 Cr, the addition of P reduces the Cr depletion and Ni enrichment. Hardening does not directly correlate with composition, but a framework for isolating the effect of hardening and segregation on cracking is suggested. The amount of void swelling in the irradiated material is shown to correspond inversely with segregation. Those alloys with greater segregation tend to swell less.

INTRODUCTION

This study analyzes the effect of alloy composition on void swelling, radiation-induced grain boundary segregation, and hardening in a series of Fe-Cr-Ni alloys. An Fe-18Cr-8Ni alloy (composition corresponding to 304 stainless steel) is used as the reference alloy for this project. AISI type 304 stainless steel is known to be susceptible to both swelling and irradiation assisted stress corrosion cracking (IASCC), where IASCC may be caused by grain boundary chromium depletion or matrix hardening during irradiation. Alloying additions are made to improve the swelling and grain boundary segregation resistance relative to 304 stainless steel.

Four compositions were studied in addition to the base alloy: Fe-18Cr-40Ni (corresponding to 330 stainless steel) and Fe-16Cr-13Ni, Fe-16Cr-13Ni+Mo, and Fe-16Cr-13Ni+Mo+P (all three corresponding to AISI 316 stainless steel). The Fe-18Cr-40Ni-alloy is studied to measure grain boundary segregation in an alloy that exhibits excellent swelling resistance. The Fe-16Cr-13Ni alloys are studied to determine the effect of major and minor element composition change between 304 and 316 stainless steel. AISI 316 is more swelling resistant [1] and more resistant to IASCC [2] than 304.

EXPERIMENT

Table 1 provides the compositions of each alloy. The Fe-18Cr-8Ni, Fe-16Cr-13Ni, and Fe-18Cr-40Ni alloys will be referred to as the Ni-series throughout this paper. The Fe-16Cr-13Ni, Fe-16Cr-13Ni+Mo, and Fe-16Cr-13Ni+Mo+P alloys will be referred to as the 316-series throughout this paper. Each alloy was cold-worked and then underwent a recrystallization anneal to obtain an average grain size of around 20 microns. Twenty-micron grains were desired because the range of damage in the proton beam used to irradiate samples is approximately forty microns. Twenty-micron grains allow the damage zone depth to cover two grains on average.

Table 1. Alloy concentrations (at%)

Alloy Designation	Fe	Cr	Ni	Mn	Mo	P
Fe-18 Cr-8 Ni	71.5	19.2	7.8	1.1	-	-
Fe-18 Cr-40 Ni	38.9	19.6	40.2	1.2	-	-
Fe-16Cr-13Ni	69.9	16.7	12.2	1.2	-	-
Fe-16Cr-13Ni+1.85Mo	68.5	16.6	12.6	1.2	1.08	-
Fe-16Cr-13Ni+1.85Mo+0.05P	68.7	16.6	12.4	1.2	1.07	0.09

Samples were irradiated using 3.2 MeV protons at 400°C to 0.5 displacement per atom (dpa) at a damage rate of $3.5x10^{-6}$ dpa/s. Following irradiation, samples were analyzed using a transmission electron microscope (TEM). The damage of the proton beam is relatively constant over the first 40 microns of penetration and the regions of the sample examined using TEM were in this flat damage region. Swelling was characterized by measuring the void size distribution in the TEM samples. Void distributions were measured using a JEOL 2010 TEM. Sample thickness for cavity density measurements was determined using convergent beam electron diffraction (CBED). Radiation-induced grain boundary segregation was measured using a Phillips CM200 field emission gun scanning transmission electron microscope (FEG-STEM). Microhardness measurements were performed on irradiated alloys to estimate the effect of irradiation on strength. Vickers hardness was measured using a Vickers Microhardness Tester (Micromet-II). A total of 30 to 50 indents at a load of 25 g were performed in both the irradiated region and the unirradiated region of the bar used for TEM sample preparation.

RESULTS

The average grain boundary segregation is plotted in Figures 1 and 2 for the Ni-series and the 316-series respectively. For alloys with relatively constant (16-19 at%) bulk chromium concentration and varying bulk nickel concentration, as the bulk nickel increases, the nickel enrichment, chromium depletion, and iron depletion all increase. For alloys with base concentration of Fe-16Cr-13Ni, the addition of molybdenum has little effect on the grain boundary segregation, but the addition of phosphorous decreases the nickel enrichment and the chromium and iron depletion.

The change in hardness is plotted in Figures 3 and 4 for the Ni-series and the 316-series respectively. For alloys with constant (16-19 at%) bulk chromium concentration and varying bulk nickel concentration, the change in hardness is smallest for the Fe-16Cr-13Ni alloy. For alloys with base concentration of Fe-16Cr-13Ni, the addition of molybdenum has little effect on the grain boundary segregation, but the addition of phosphorous increases hardness.

The void swelling is plotted in Figure 5 for the Ni-series. For alloys with constant (16-19 at%) bulk chromium concentration and varying bulk nickel concentration, the void swelling decreases with increasing bulk nickel. Void distributions are not yet complete for the 316 series.

DISCUSSION

Radiation-induced segregation and swelling

Previous work has shown that changes in bulk composition can reduce void swelling by increasing the average vacancy diffusivity (to reduce the void nucleation rate) and by decreasing the vacancy diffusivity near the void surface due to RIS (to reduce the void growth rate) [3]. The changes in the shear modulus and lattice parameter caused by RIS near a void surface also affect the ability for voids to nucleate and grow. Wolfer et al. showed that a compositional change which increases the shear modulus or lattice parameter locally around a void embryo causes the void to become a preferential sink for vacancies, thus increasing the void nucleation rate [4-6]. For Fe-Cr-Ni alloys with compositions near 304/316 stainless steel, the lattice parameter and shear moduli increase with increasing Cr concentration and decrease with increasing Ni concentration [4]. For 304/316 stainless steel, RIS causes Cr to deplete and Ni to enrich around a void during irradiation. These changes in lattice parameter and shear modulus would tend to mitigate void nucleation. The smaller void density for alloys with greater bulk nickel concentration support the contention that increased RIS mitigates void nucleation.

Radiation-induced segregation, hardness, and IASCC

Two effects of radiation on microstructure have been hypothesized to contribute to IASCC: Cr depletion leading to decreased grain boundary corrosion resistance and matrix hardening leading to a grain boundary weakened relative to the matrix. Support for the matrix hardening contribution was provided by Was and Bruemmer who showed that IGSCC susceptibility correlated reasonably well with increasing yield stress [7]. Additionally, 316 has a greater stacking fault energy than 304, making dislocation channeling easier, possibly leading to a concentration of stress at the grain boundary and an increased probability of grain boundary cracking. Yet 316 is typically less susceptible than 304 to IASCC [2]. Cookson et al. found that increasing Ni content decreased IASCC susceptibility [8].

Comparing the Fe-18Cr-8Ni (corresponding to 304 stainless steel) and Fe-16Cr-13Ni (corresponding to 316 stainless steel) alloys, moving toward the 316 composition causes decreased hardening (Figure 3) and greater Cr depletion (Figure 2). Decreased hardening (and the corresponding decrease in yield strength) should decrease cracking susceptibility. Greater Cr segregation should make 316 more susceptible to IASCC. The hardness measurements and segregation measurements do not clearly indicate property changes that would make 316 stainless steel more susceptible than 304. The hardening and segregation in the 316-series are not significantly affected by the addition of molybdenum. The addition of P increases hardening and decreases chromium depletion. The increased hardening should correspond to an increased IASCC susceptibility while the decreased chromium depletion should decrease IASCC susceptibility. . The hardness measurements and segregation measurements do not clearly indicate property changes that would make Fe-16Cr-13Ni stainless steel with the minor elements included more susceptible than base Fe-16Cr-13Ni.

Figure 6 plots the change in yield strength versus the grain boundary chromium depletion for all five alloys in this study. The yield strength change is calculated from the measured hardness using the following correlation:

$$\Delta\sigma_y = K\Delta H_v. \qquad (1)$$

When yield strength is measured in MPa and hardness is measured in HV (kg/mm^2), the conversion factor K for alloys corresponding to 304 stainless steel (Fe-18Cr-8Ni) is 3.48 and the conversion factor K for alloys corresponding to 316 stainless steel (Fe-16Cr-13Ni) is 3.27 [9]. The graph is divided into four quadrants. Of the five alloys studied, three clusters arise. The Fe-16Cr-13Ni and Fe-16Cr-13Ni+Mo alloys have lower hardening and greater chromium depletion, the Fe-18Cr-8Ni and Fe-16Cr-13Ni+Mo+P alloys have higher hardening and lower chromium depletion. The Fe-18Cr-40Ni alloy has greater hardening and greater chromium depletion. Stress corrosion cracking tests of these alloys should provide an indication on the relative importance of hardening and chromium depletion.

CONCLUSIONS

Void swelling, hardening, and radiation-induced segregation have been studied in five austenitic stainless steel alloys (Fe-18Cr-8Ni, Fe-16Cr-13Ni Fe-16Cr-13Ni+Mo, Fe-16Cr-13Ni+Mo+P, and Fe-18Cr-40Ni). Increasing the bulk nickel concentration decreases void swelling and increases grain boundary chromium depletion and nickel enrichment. Hardness increases during irradiation do not track with bulk nickel content. For alloys based on the composition Fe-16Cr-13Ni, the addition of molybdenum has little effect on hardening or segregation. The addition of P increases hardening and decreases segregation. Analysis of the data indicates that radiation-induced segregation to void surfaces correlates with reduced void swelling. One mechanism for this reduction in swelling may be the reduction in lattice parameter and shear modulus that occurs due to RIS. Plotting the hardening versus chromium depletion indicates that different alloys respond to irradiation in clusters. Some clusters have higher hardening and less segregation, others have lower hardening and greater segregation. Because of the natural clustering, stress corrosion cracking testing should elucidate the influence of hardening and segregation on intergranular cracking behavior.

ACKNOWLEDGEMENTS

Research at the Oak Ridge National Laboratory SHaRE Collaborative Research Center was sponsored by the Division of Materials Sciences and Engineering, U.S. Department of Energy, under contract DE-AC05-00OR22725 with UT-Battelle, LLC, and through the SHaRE Program under contract DE-AC05-76OR00033 with Oak Ridge Associated Universities. Work supported under contract W-31-109-Eng-38 with the Department of Energy.

REFERENCES

1. F. A. Garner, in Materials Science and Technology, A Comprehensive Treatment, Vol 10A Nuclear Materials, Edited by R. W. Cahn, P. Haasen, and E. J. Kramer, (VCH Weinheim, 1994).
2. Y. Tanaka, S. Suzuki, M. Kodama, S. Nishimura, K. Fukuya, H. Sakamoto, K. Nakata, and T. Kato, *Proceedings of the Eighth International Symposium on Environmental Degradation of Materials in Nuclear Power Systems-Water Reactors*, (American Nuclear Society, 1997), p.803.
3. T.R. Allen, J.T. Busby, J. Gan, E. A. Kenik, G.S. Was, *Effects of Radiation on Materials: 19th International Symposium, ASTM STP 1366*, Edited by M. L. Hamilton, A. S. Kumar, S. T. Rosinski, and M. L. Grossbeck, (American Society for Testing and Materials, West Conshohocken, PA, 2000), p. 739.
4. W. G. Wolfer, F. A. Garner, et al. *Effects of Radiation on Materials: Eleventh Conference, ASTM STP 782*, (American Society for Testing and Materials, 1982) p.1023.
5. W. G. Wolfer and L. K. Mansur, J. Nucl. Mater. **91** 265 (1980).
6. A. Si-Ahmed and W. G. Wolfer *Effects of Radiation on Materials: Eleventh Conference, ASTM STP 782, American Society for Testing and Materials* (1982), p.1008.
7. G. S. Was and S. M. Bruemmer, J. Nucl. Mater., **216**, 326 (1994).
8. J. M. Cookson, D. L. Damcott, G. S. Was, and P. L. Andresen, *Proceedings of the 6th International Symposium on Environmental Degradation of Materials in Nuclear Power Systems-Water Reactors*, San Diego, CA (1993), p. 573.
9. H. R. Higgy, F. H. Hammad, J. Nucl. Mater., 55 (1975) 177.

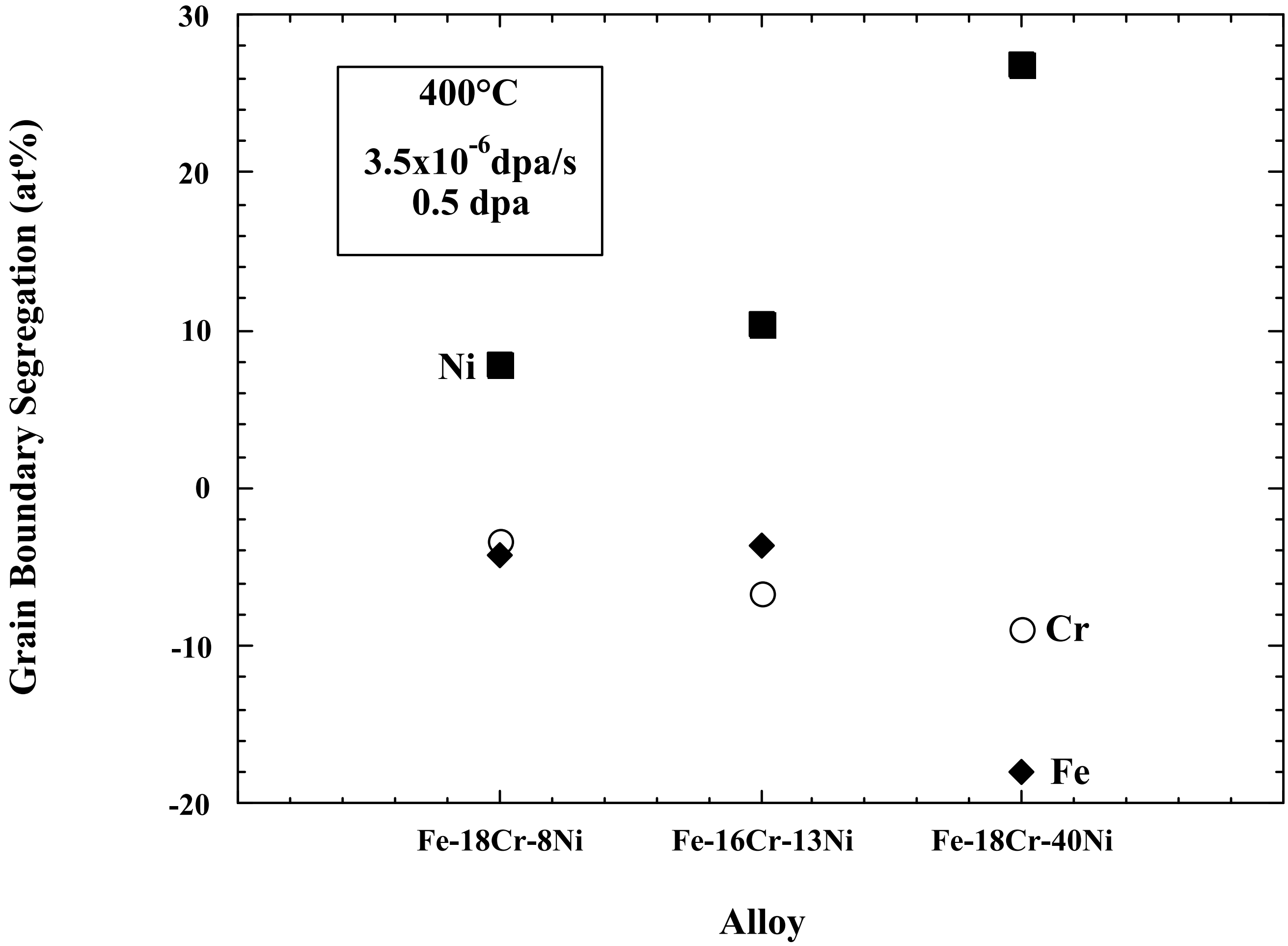

Figure 1. Grain boundary segregation as a function of alloy composition for the Ni-series.

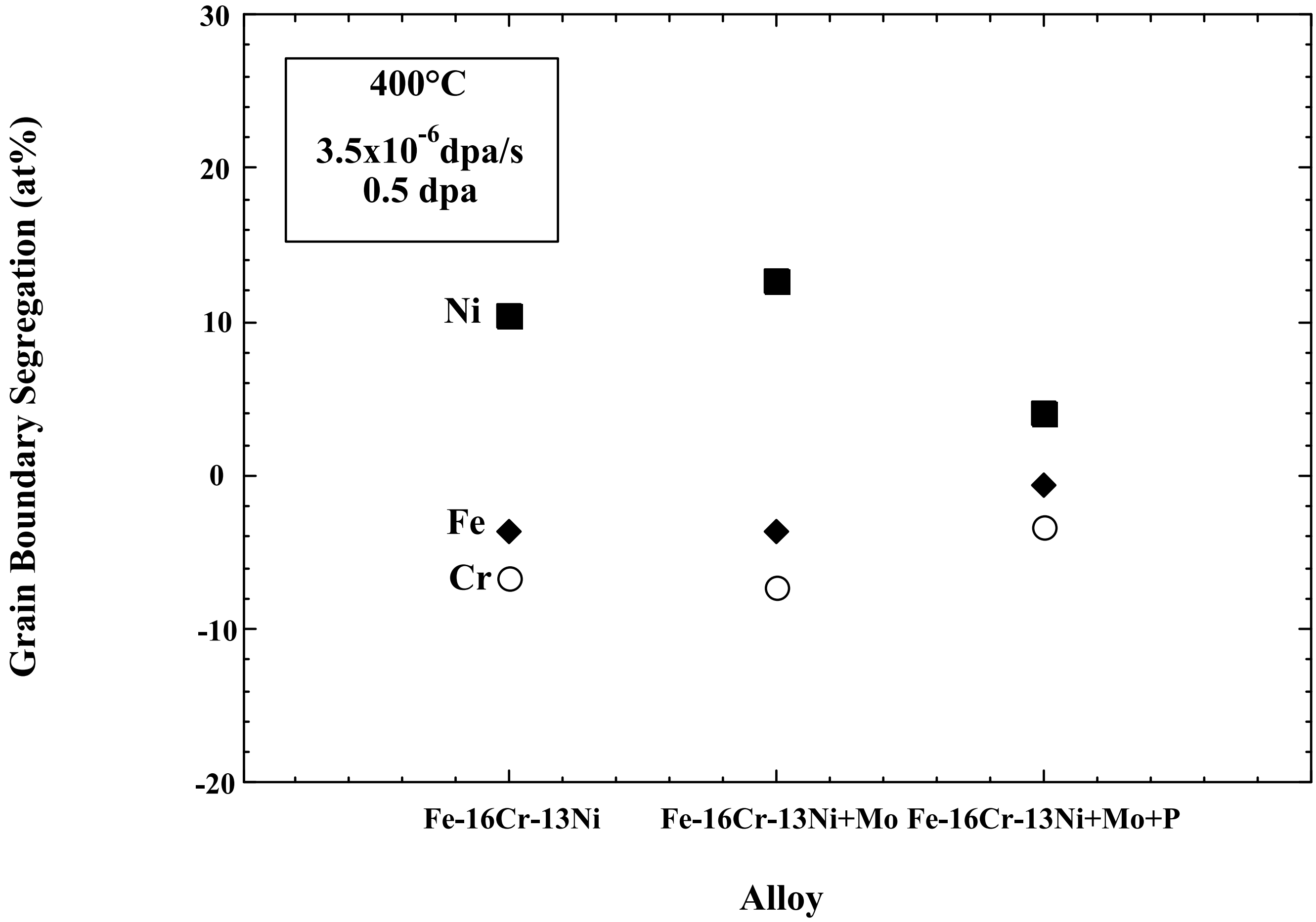

Figure 2. Grain boundary segregation as a function of alloy composition for the 316 series

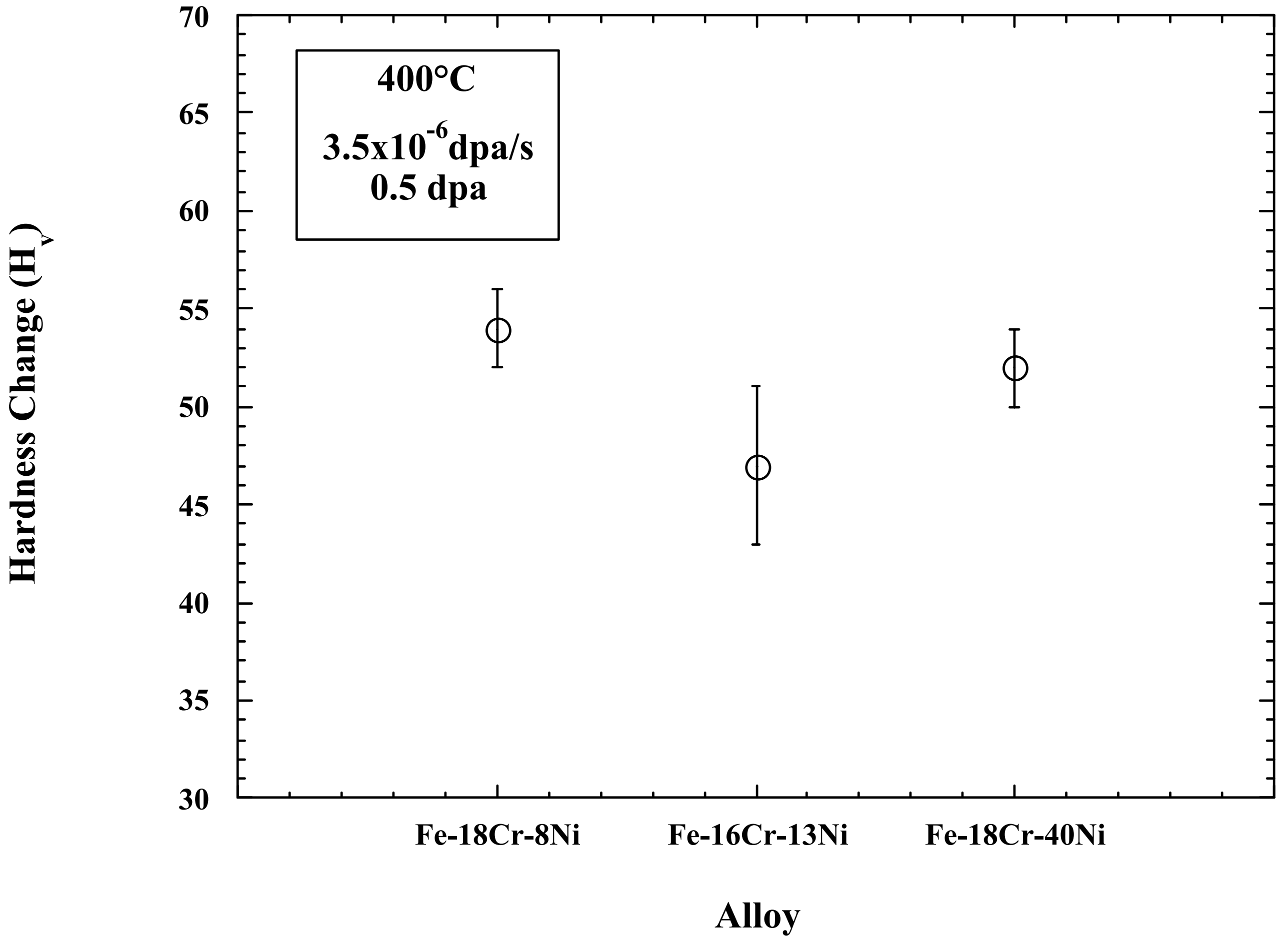

Figure 3. Hardness as a function of alloy composition for the Ni-series.

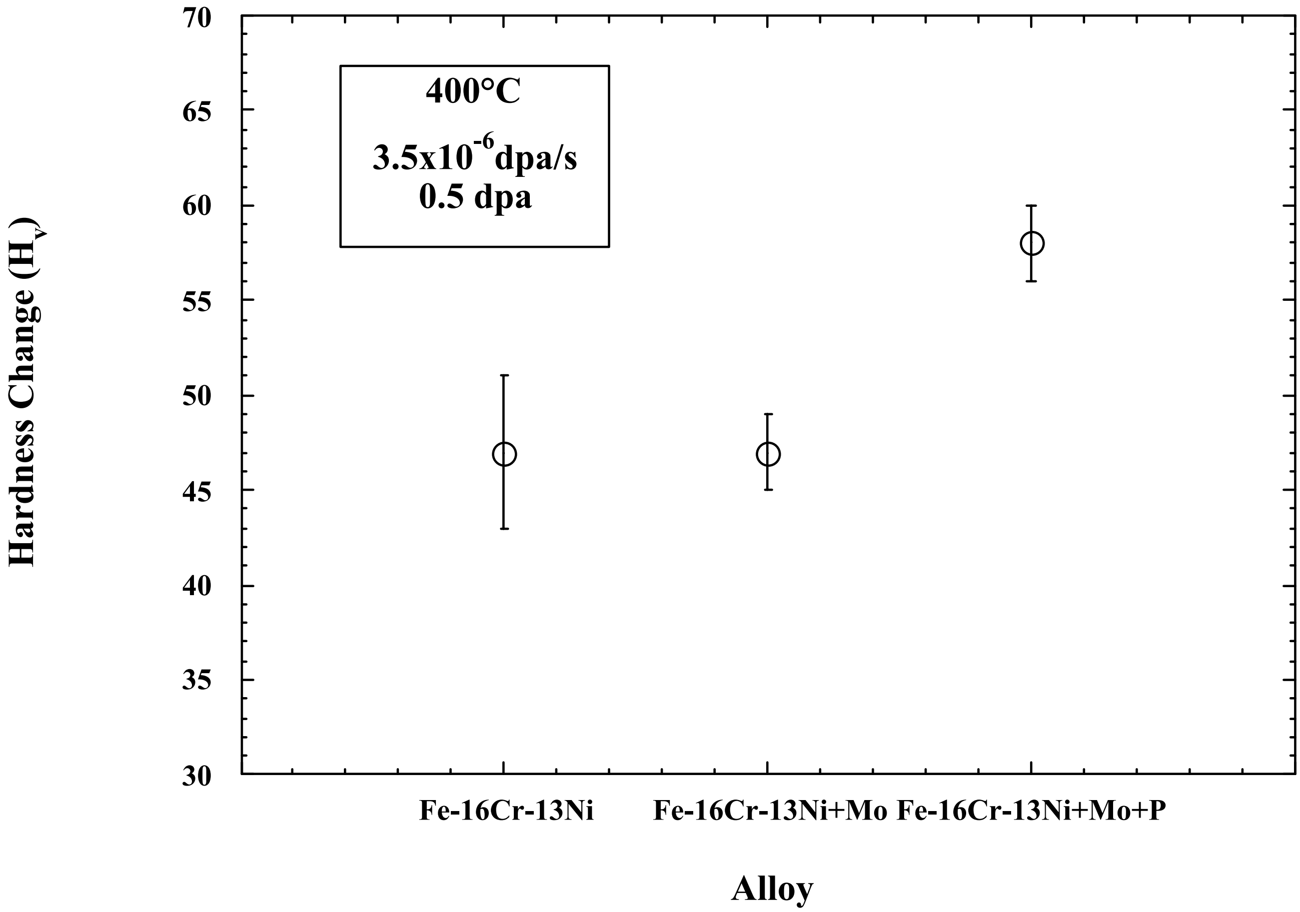

Figure 4. Hardness as a function of alloy composition for the 316 series.

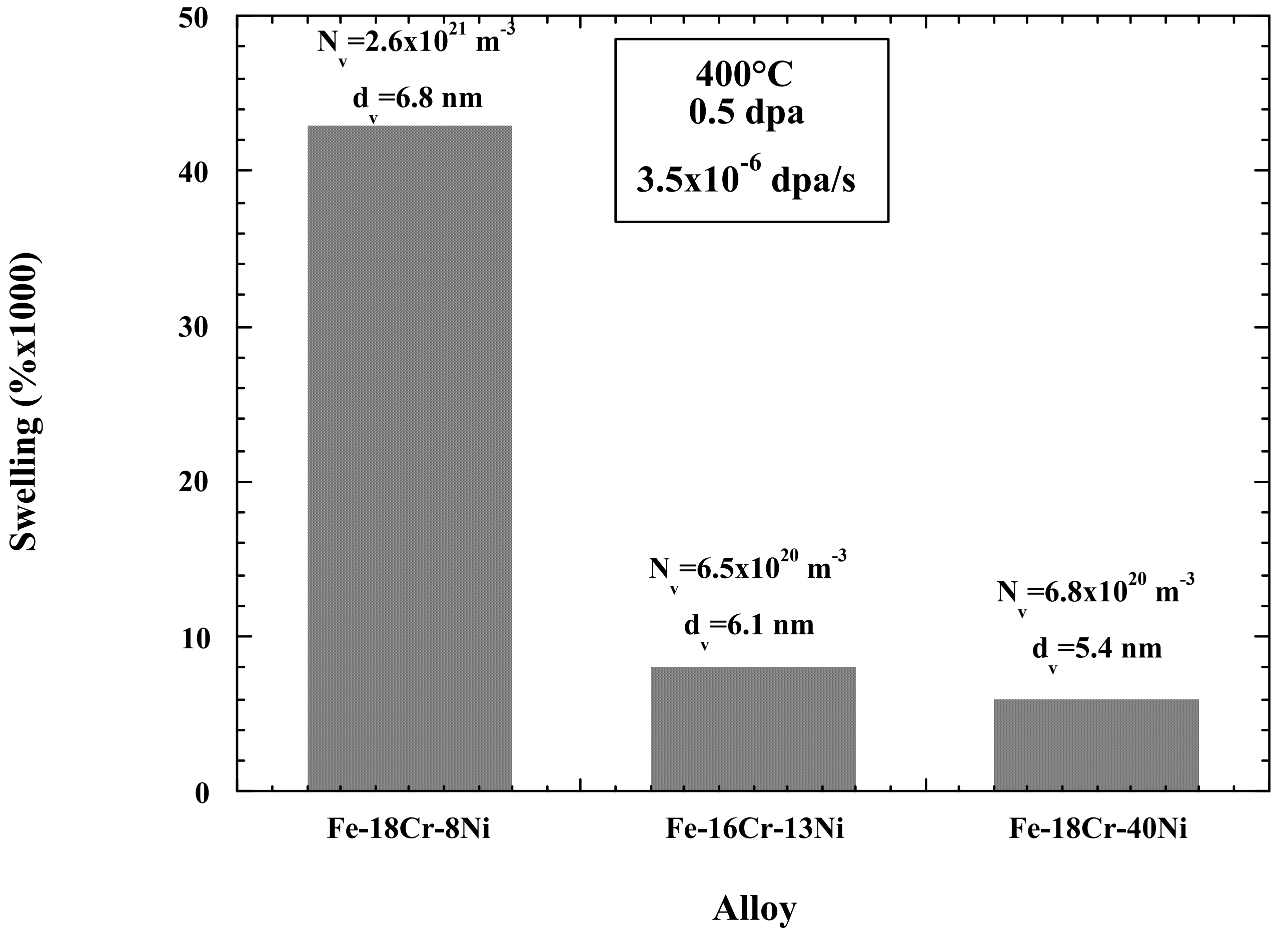

Figure 5 Void swelling as a function of composition for the Ni-series

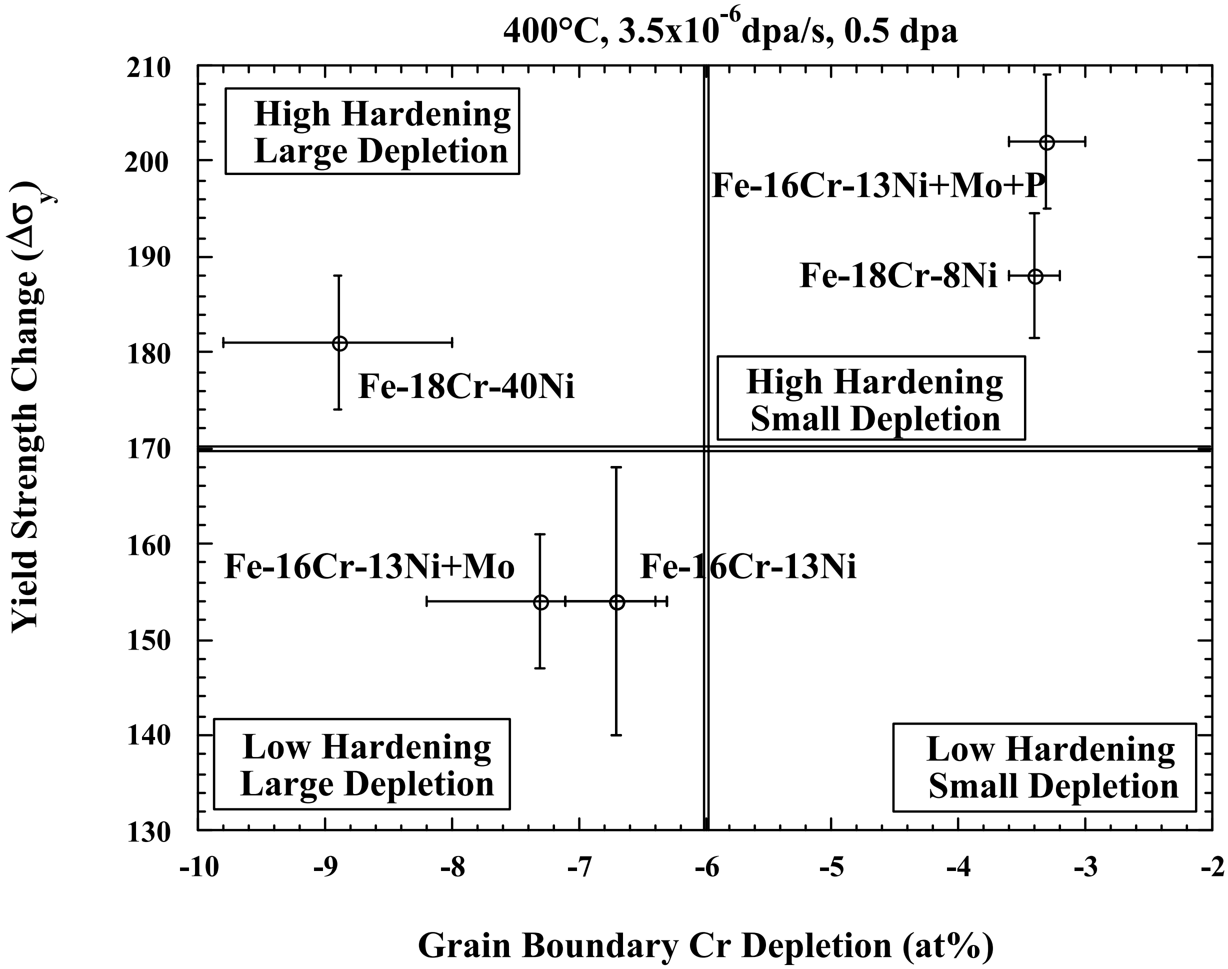

Figure 6. Hardening and depletion regions.